ELSEVIER

Sensors and Actuators A 57 (1996) 1–8

SENSORS AND ACTUATORS A PHYSICAL

Digital stochastic magnetic-field detection [1]

Siegbert Hentschke

IPM, Kassel University, 34109 Kassel, Germany

Received 19 December 1995; revised 19 April 1996; accepted 4 June 1996

Abstract

The objective of this project is the improvement of magnetic-field detection for parallel data reading. In this paper a new type of sensor for magnetic-field measuring is presented, which allows the detection or measurement of magnetic fields on square-micrometre areas with a flexible sensitivity. This performance is achieved by specially designed CMOS MAGFET structures that directly digitize the Hall field at the point of measurement, hence avoiding further analogue gain noise disturbances. It is shown which stochastic evaluations lead to millitesla resolutions on square-micrometre regions in the microsecond range and to microtesla resolutions in intervals of seconds. Some prototypes of digitizing stochastic MAGFET cells have been fabricated. The principal layout structures of cells are shown. An impact on future data-recording improvement is predicted if digital data-track adaptation methods are implemented into integrated digital reading heads.

Keywords: Magnetic-field detection; Stochastic methods

1. Preface

Activities concerning the design of integrated (intelligent) magnetic-field detectors are manifold: by making use of the Hall effect, suitable materials characterized by high electron mobility, such as GaAs, are being developed and manufactured [1–3]. For commercial purposes, Si technologies are being favoured [4,5]. The principle of magnetic-field transistors (MTs) with two collectors and adequate field-effect transistors (MAGFETs) has been known for more than a decade now; different kinds have been scanned and analysed [3,7]. In 1986 Baltes and Popovic [7] presented a survey of the physical state-of-the-art. In the meantime, many types of magnetic-field sensors (MFSs) have been manufactured in an integrated manner, have been scanned, and comparative analyses of performance features relating to noise characteristics and temperature dependency have been undertaken, for standard Si processes as well.

The buoyantly expanding industry of magnetic bulk-storage devices now employs silicon-based semiconductive magnetic heads [5]. An increase in detection speed, in sensitivity and, above all, in the scale of integration is of utmost interest today. Usually, analogue data acquisition of magnetic signals is followed by digital processing. Hence, low-noise, sensitive transistor switches are required [4], in order to allow for conversion to digital signals in conventional A/D converters. If it were possible to shift digitization further right to the sensor, slightly more digital logic would solve many an analogue problem. The present article shows how this is possible. Particularly, sub-micron technologies will probably induce increased complexity, which will open up new classes of sensors with performance features yet unknown: arrays made up from multiple optimized magnetic-field sensor cells with the capability to scan minute magnetic fields multidimensionally. A wide range of applications is feasible: from positioned alignment and scanning in mechanics and robotics to data storage and video engineering.

As the many developments and results show, process engineering is now due for integrated solutions of magnetic-field sensors. What is still needed is the development of basic cells for specific purposes, which will then be integrated into a digital or analogue circuit environment on a (CMOS, Bi-CMOS or GaAs) chip. The present paper will illustrate the principle of a digital magnetic-field detector, the layout cell of which can easily be interconnected to the existing digital logic. Signal-theoretically the digitizing decisions for magnetic-field detection are to be shifted toward the micro area of measurement as much as possible, in order to prevent additional transistor gain noise. This can be achieved by creating a highly unstable state in the semiconducting area in which the magnetic field is to be detected. This is done in such a manner that even the slightest imbalance in the charge distribution will lead to the tilting into one out of two (or

[1] Dedicated to Professor Dr rer.nat. Josef Hoschek, TH Darmstadt, on the occasion of his 60th birthday.

PII S0924-4247(96)01326-X

more) possible states of stability. After saving this one-bit information, a new unstable decision state can be created. This scanning procedure is conducted at the highest clock frequency possible. Due to the fact that the unstable order demands a decision, in the best of cases the thermally induced random electron movement will suffice for a decision, then allowing for stochastic evaluation of the one-bit information thus gained. It is possible, however, to describe precisely the random electron behaviour with respect to the different effects causing it. Thus, even small variations in the expected frequency distribution indicate the influence of a magnetic field. So far, most publications have calculated the limits of sensitivity by comparing the magnetic-field-induced deviation of the measured variable with the effective value of the superimposed noise. Specific stochastic analysis, however, enables us to give a measurable value much smaller than that of the superimposed noise.

2. Introduction

The law of physics that allows for the tracing of the existence of a stable magnetic field in a semiconductor is the formation of the Lorentz force $\boldsymbol{F}_L$ on an electrical charge q_e, moving relative to a magnetic field $\boldsymbol{B}$ at the speed $\boldsymbol{v}$:

$$\boldsymbol{F}_L = q_e \cdot (\boldsymbol{v} \times \boldsymbol{B}) = q_e \cdot \boldsymbol{E}_H \quad (1)$$

where $\boldsymbol{E}_H$ represents the equivalent Hall electric-field intensity.

With fast-changing magnetic fields, such as those created by rotating mass-storage media, forces also affect resting charges in the semiconducting material, which corresponds to the law of induction in the Maxwell field equation:

$$\nabla \times \boldsymbol{E}_m = -\frac{\partial \boldsymbol{B}}{\partial t} \quad (2)$$

The Boltzmann transport equations describe the currents in the semiconductor for positive and negative charges. Let us first restrict our analysis to n-conducting materials (i.e., the transport of negative electron charges) in an isotropic temperature-gradient-free material: we obtain the following charge density $\boldsymbol{J}_{ED}$, induced by the electrical field and the space-charge gradient:

$$\boldsymbol{J}_{n,ED} = \boldsymbol{\sigma}_n \cdot \boldsymbol{E} + qD_n \cdot \nabla n \quad (3)$$

$\sigma_n = q\mu_n n$ stands for the electrical conductivity of the material in the case $\boldsymbol{B} = \boldsymbol{0}$, whereas $\boldsymbol{E}$ describes the electrical-field density in the material, $q = 1.6 \times 10^{-19}$ A s the charge of an electron, $D_n = \mu_n kT/q$, $n = N(\boldsymbol{x})$ the location-dependent electron density and μ_n the electron mobility parameter. If a magnetic field $\boldsymbol{B}$ comes into existence, the current density will be superimposed by that part of the current density superimposed by the Lorentz force:

$$\boldsymbol{J}_n(\boldsymbol{B}) = \boldsymbol{J}_{n,ED} + \mu_n^* \cdot [\boldsymbol{B} \times \boldsymbol{J}_n(\boldsymbol{B})] \quad (4)$$

with μ_n^* stipulating the Hall electron-mobility constant. For most semiconductors the Hall mobility is located within close range of the mobility parameter μ_n, being given by $\mu_n^* = \mu_n r_n$. The scattering constant r_n is achieved as follows from the estimated values expected for the free displacement times τ_n between electron collisions: $r_n = E[\tau_n^2]/E^2[\tau_n]$. Eq. (4) can be solved recursively taking convergence into account. For small and medium-sized doped concentrations it is also possible to give a closed solution:

$$\boldsymbol{J}_n(\boldsymbol{B}) = [\boldsymbol{J}_{n,ED} + \mu_n^* \boldsymbol{B} \times \boldsymbol{J}_{n,ED} + \alpha \cdot \boldsymbol{B}] \times \left[\frac{1}{1 + (\mu_n^* B)^2}\right], \quad \alpha = (\mu_n^*)^2 (\boldsymbol{B} \cdot J_{n,ED}) \quad (5)$$

Hence, the equation given describes the transport of negative charges in the presence of stationary electrical and magnetic fields. For the transport of positive charges, i.e., electron holes, an analogous relation is valid.

In the simplified case, location-dependent changes in the charge density being rather small and the magnetic-field intensity occurring perpendicular to the electrical one, the following fundamental part of the current density remains:

$$\boldsymbol{J}_n = \sigma_n [\boldsymbol{E} + \mu_n^* \cdot (\boldsymbol{B} \times \boldsymbol{E})] \beta; \quad \beta = \frac{1}{1 + (\mu_n^* \boldsymbol{B})^2} \quad (6)$$

Let the common part of the n-channel of the double-drain FET (cf. Fig. 1) be of length l and thickness d, resulting in the area $A = ld$. The current through this area multiplied by the switching time T gives an estimation of the electron-charge difference ΔQ flowing perpendicular within the channel and initiating the fall into one of the two possible stable situations after the opening of the common channel by the clock during the time T:

$$\Delta Q = (\boldsymbol{J}_n \cdot \boldsymbol{e}_t) TA = \sigma_n \mu_n^* |\boldsymbol{B} \times \boldsymbol{E}| \beta TA \quad (7)$$

The vector $\boldsymbol{e}_t$ denotes the perpendicular channel direction, which can be assumed to be orthogonal to $\boldsymbol{B}$ and $\boldsymbol{E}$. Fig. 1 shows the layout of two types of double-drain MAGFETs: (a) is a standard type having the two drains serially in line with the gate and (b) having the two drains lateral to the gate to achieve a gate of smaller width d. The influencing magnetic field B appears perpendicular to the gates.

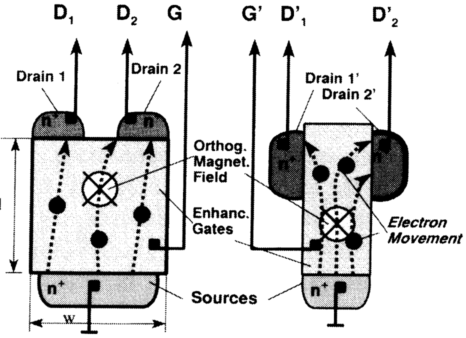

Fig. 1. Layout structure of two double-drain MAGFETs with enhancement gate channels.

3. Stochastic evaluation of binary detections

The decisions of the binary detector coming out of the unstable state and going into one of two possible states follow strong stochastic rules. The relevant time for the decisions might be a small interval appearing directly after the clock rise. If no magnetic field is present the decisions follow the random charge differences of electrons under the gate due to thermal fluctuations. Let the double-drain MAGFET be of totally symmetric structure; then, on average, both decisions are equally distributed. In this case the thermal charge bias ΔQ during the decision phases of a large number of decisions will have an average value of zero: $\langle \Delta Q \rangle = 0$. Therefore the deviation probability ΔP of the right decision P_+ from 0.5 will be zero: $P_+ + \Delta P = 0.5$; $\Delta P = 0$. But while a steady orthogonal magnetic field goes through the channel, the probability for a right (respectively, left) decision increases due to repeated charge biases ΔQ, caused by the expectation (or average value) $\langle \Delta Q(B) \rangle$ which is proportional to the absolute value of B: $\langle \Delta Q(B) \rangle \sim |B|$. Let ΔQ_{eff} be the standard deviation of fluctuations due to the thermal noise appearing directly after channel opening by the clock. A constant small magnetic field B_0 may cause a constant $\langle \Delta Q(B_0) \rangle$. Then the probability bias ΔP will be proportional to $|B_0|$ over the standard deviation ΔQ_{eff}: $\Delta P \sim |\langle \Delta Q \rangle| \Delta Q_{\text{eff}} \sim |B_0| / \Delta Q_{\text{eff}}$. In the following this relationship will be calculated in more detail. After L decisions the probability distribution will be binomial; because of the thermal noise there is no correlation between the two decisions:

$$P_{B\pm}(j; L) = \binom{L}{J} P_+^j P_-^{(L-j)} \quad (8)$$

During each clock period a '−' or '+' decision occurs. For convenience, a '+' decision is represented by '1' and a '−' decision by '0'. If, over an interval of L clock periods, s '+' decisions have been counted, the complementary number of $L-j$ '−' decisions have consequently taken place. Now let $P_+ = 0.5 + \Delta P$ be the probability of a '+' decision. The probability that just s '+' decisions occur during the interval of L periods is then given by the binomial distribution

$$P_B(j=s) = \binom{L}{s} P_+^s P_-^{(L-s)}$$

$$= \binom{L}{s} (0.5 + \Delta P)^s (0.5 - \Delta P)^{L-s} \quad (9)$$

Because only binary '+' and '−' decisions are allowed, the probability for one decision P_- is complementary: $P_- = 1 - P_+$.

When no magnetic field is present the probabilities for '+' and '−' decisions, of course, must be equally distributed: $P_+(B=0) = P_-(B=0) = 0.5$, or $\Delta P(B=0) = 0$. Therefore we will substitute $P_+ = 0.5 + \Delta P$. In general the expectation E and the variance V of the above-mentioned binomial distribution (Eq. (9)) after L decisions will be:

$$E\{j\} = L\left(\frac{1}{2} + \Delta P\right) \quad V\{j\} = \frac{L}{2}[1 - (2\Delta P)^2] \quad (10)$$

It is more convenient and reasonable to use a bias counter for the decision counting rather than counting the events separatly. This is an up/down counter that counts +1 for a '+' decision and −1 for a '−' decision; in some extraordinary cases that might happen from time to time when the time for a decision was too short, the bias counter can hold the old number, which means the counting of a zero. In this way the 'no-decision events' can be tolerated. For further calculations the '0' decision will not be taken into account. Let b be the number of such a bias counter that ranges between $-L$ and $+L$, i.e., $-L \le b \le L$. Using b instead of j in Eq. (8) (or Eq. (9)) gives the substitution $b = 2j - L$ or $j = (b+L)/2$.

The binomial distribution is expressed by:

$$P_B(b) = \binom{L}{\frac{b+L}{2}} P_+^{\frac{b+L}{2}} P_-^{\left(L - \frac{b+L}{2}\right)}$$

$$= \binom{L}{\frac{L+b}{2}} \left(\frac{1}{2} + \Delta P\right)^{\frac{b+L}{2}} \left(\frac{1}{2} - \Delta P\right)^{\frac{L-b}{2}} \quad (11)$$

The expectation of the bias counter and the variance as a function of ΔP and L then equal

$$E\{b\} = 2\Delta P L \quad V\{b\} = L(1 - (2\Delta P)^2) \quad (12)$$

For a large number of decisions L and small ΔP the binomial distribution function for b converges towards the following continuous Gauss distribution function:

$$p(b) \approx \frac{1}{\sqrt{2\pi L}} \exp\left[-\frac{1}{2} \frac{(b - 2\Delta P L)^2}{L}\right] \quad (13)$$

The decisions in the detection device are generated by an unbalanced flow of electrons through a double-drain MAGFET enhancement channel which is opened by the voltage of a joint gate (see Figs. 1 and 3). The longitudinal drift movements of electrons through the channel get a transversal component from the orthogonal magnetic field B. The equivalent transversal electric field is given by $E_t(B) = v_e B_o$, with v_e being the average velocity of electrons and B_o the magnetic field orthogonal to the joint gate. The symmetric flow arriving in the two drains is disturbed by the thermal movement of the electrons, which is unpredictable and independent from any period to another. It is a white noise and can be described by a Gaussian distribution having the random voltage u and the effective alternating voltage σ. This decision-producing probability distribution function is then

$$p(u)=\frac{1}{\sigma\sqrt{2\pi}}\exp\left[-\frac{1}{2}\left(\frac{x}{\sigma}\right)^2\right]$$
$$=\frac{1}{\sigma\sqrt{2\pi}}\exp\left[-\frac{1}{2}\left(\frac{u-\delta u_B}{\sigma}\right)^2\right] \quad (14)$$

where $\delta u_B=\alpha B_o=\mu_G v_e B_o l$ is estimated to be the equivalent average bias voltage and μ_G is a channel geometry coefficient arising from short-circuit effects and different charge densities in the channel, which are discusssed later. The value of the noise voltage σ will also be discussed in more detail later under sensitivity estimation. The above distribution function means for the decisions that if the random voltage $u>\alpha B_o$ a $+1$ is counted by the bias counter b and elsewhere a -1 is counted. A small probability deviation ΔP from 0.5 is expressed by the following integral:

$$\Delta P=\frac{1}{\sigma\sqrt{2\pi}}\int_{u=0}^{\alpha B_0}\exp\left[-\frac{1}{2}\frac{(u-\alpha B_o)^2}{\sigma^2}\right]\mathrm{d}u \quad (15)$$

For this integral an approximation can be used for small values of ΔP:

$$\Delta P\approx\frac{\alpha B_o}{\sigma\sqrt{2\pi}}\exp\left[-\frac{1}{2}\left(\frac{0.6\alpha B_o}{\sigma}\right)^2\right] \quad (16)$$

The chosen x-axis representation $0.6\alpha B$ is a suitable value which has been proved by simulation to make this approximation not only suitable for very small values of B but also gives practical approximations up to $\alpha B<\sigma$.

For our measurement purposes ΔP is given and B has to be determined from Eq. (16). This can be done iteratively. The first iteration derived from the formula above is given by the following equation, which can be used to find the first iteration value of B:

$$B_{(0)}=\frac{\sigma}{\alpha}\Delta P\sqrt{2\pi} \quad (17)$$

This estimation already holds for very small values of B. For bigger values the following first-order iteration will be used:

$$B_{(1)}=\frac{\sigma\Delta P}{\alpha}\sqrt{2\pi}\exp\left[\frac{1}{2}\left(0.6\alpha\frac{B_{(0)}}{\sigma}\right)^2\right]$$
$$=\frac{\sigma\Delta P}{\alpha}\sqrt{2\pi}\exp[\pi(0.6\Delta P)^2] \quad (18)$$

It has to be mentioned again that this formula starts from an approximation for small ΔP. Let b be the number of the bias counter after L decisions or clock periods. According to Eq. (12) the probability deviation ΔP is measured by the bias counter: $\Delta P=b/(2L)$. The two device-specific constants α and σ can be put together conveniently into $\beta=\sigma/\alpha$. This parameter β will have directly the dimension of tesla [T]. For $B<\beta$ the estimation for magnetic field is derived from Eq. (18). Hence substituting ΔP we get

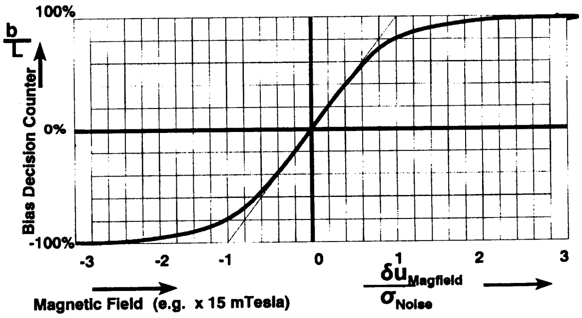

Fig. 2. Characteristic of a digital stochastic magnetic-field sensor: b = bias counter number; L = number of measuring periods.

$$B=\frac{\beta b}{2L}\sqrt{2\pi}\exp\left[\pi\left(0.3\frac{b}{L}\right)^2\right] \quad (19)$$

This description holds for small values of b/L. To cover the whole range, the Gaussian integral can be applied as the error function for an accurate description. For this let

$$Y=\mathrm{erfc}(X)=\int_0^X\frac{1}{\sqrt{2\pi}}\exp\left(-\frac{1}{2}x^2\right)\mathrm{d}x \quad (20)$$

Using this notation the final result to detect the magnetic field B by the number of the bias counter b after L clock periods is given by

$$B=\beta\,\mathrm{erfc}^{-1}\left(\frac{b_0}{2L}\right) \quad (21)$$

where b_0 denotes the final position of the binary counter after L clock periods. This function finally defines the characteristic of an ideal digital stochastic MAGFET device. In practice each device will have some slightly different characteristics dependent on geometry coefficients which have not been considered here. Fig. 2 shows that the function is rather linear for $|B/\beta|<1/2$ and that for higher fields the linear relationship has to be corrected by the inverse error function shown above. For $|B/\beta_0|>2$ the useful range is practically limited. In case wider ranges are wanted, the MAGFET device can be controlled by an electronic shifting of the symmetry, which is not discussed here.

3.1. Accuracy, resolution and confidence interval of results

The field has to be measured over a period of L clock intervals. It is assumed that the field to be measured is relatively constant. The method most often used to get information on the confidence level of an unknown variable is to store the numbers of the measured variable (the bias counter) of fixed partitioned intervals and the estimate from these step values between the confidence interval. For example, the interval of 1000 clock periods could be divided into 10 steps of 100 when the positions of the bias counter are stored. But the occurring binomial distribution function has well-known stochastic moments. As already described in Eq. (12), the standard deviation of the bias counter after L clock periods is $s=[L(1-(b/L)^2]^{172}$. Let us take into account only relatively small values of b, i.e., $|b/L|<1$. Then the percentage of correct samples belonging to an interval of the standard deviation s around a counted value b_0 can be calculated by the Gaussian error function: about 68% of repeated measurements will belong to the interval, while about 95% will belong to the doubled interval $b_0 \pm 2s$. For convenience we will use the standard deviation as sufficiently accurate notation. Taking into account small values, the 68% confidence interval notation is the following

$$B=\frac{\beta}{L}\sqrt{\frac{\pi}{2}}(b_0 \pm \sqrt{L}) \tag{22}$$

If the whole range has to be covered, the equivalent notation is

$$B=\beta \mathrm{erfc}^{-1}\left\{\frac{b_0 \pm \sqrt{L\left[1-\left(\frac{b_0}{L}\right)^2\right]}}{2L}\right\} \tag{23}$$

The bit accuracy of B, of course, depends on the measuring interval L. If the full position of the bias counter were stored then a lot of irrelevancy would be included. Therefore a reasonable quantization should be made to store or to transmit only the relevant part. If a quantization interval equal to the standard deviation s is used, then a quantization power of $(s/2)^2/3$ is randomly produced. This is just 1/12 of the equivalent noise power s^2 contained in the measurement information of the bias counter. Hence, according to Shannon's theorem real information of $[\log_2(1+1/12)]/2=0.12$ bit is lost per quantization sampling, which is quite acceptable. In this case the LSB (least significant bit) will carry the measurement information of $[\mathrm{ld}(1+1/3)]/2-0.12$ bit $=0.33$ bit. The remaining 0.67 bit is noise or irrelevancy. Thus the bias counter is quantized by intervals of the standard deviation size s: $I_Q=\{x|-s/2+b_0<x<b_0+s/2\}$. Mathematically this quantization is equivalent to

$$b_{0Q}=\mathrm{int}\left[\frac{2b_0}{\sqrt{L}}+0.5\right] \tag{24}$$

where 'int' is the integer function that gives, e.g., the interval from 0 to 1 into the number 1. The logical operation for this quantization is done very easily: counting up to a number $L=2^{4n}+2^n$ and cutting the $2n-1$ LSBs of the bias counter. Taking into account '+' and '−' values of the bias counter, the remaining efficient word length will be $2n+2$ bits.

The non-linearity needs to be corrected. Looking at the sensor characteristic in Fig. 2 we see that the quantized value b_{0Q} is not proportional to the magnetic field B. The usable range for B is increased a little bit by this non-linearity: $-2\beta<B<2\beta$. After the correction of the quantized bias counter number, the bit word length has to be increased by one bit to present the limit values of $B_1=2\beta$. This results in the following accuracy statement:

The measured values of a magnetic field with a digital stochastic MAGFET device is represented by $2n+3$ bit for a measurement interval $L=2^{4n}+2^n$.

For instance, let $\beta=15$ mT and let the digitization device run at a clock frequency of 16 MHz. Then every second a 15-bit signal can be displayed covering a range from 5 μT to 30 mT.

3.2. Binary data detection

One of the main application fields for the digital stochastic MAGFET device is data reading from disks or tapes. For such purposes a low bit error rate (BER) is necessary. To achieve a reading BER $<10^{-8}$ a signal-to-noise ratio S/N $=6$ is needed (a further decrease of the BER can be achieved by error-correcting codes). For this accurate detection the quantized bias counter has to reach the absolute number six on average because the confidence level of the LSB itself is far too low. For instance, if a magnetic data field of magnitude $B=\pm\beta$ has to be detected, a minimal number of 45 decisions is required on average to reach the position ± 6 of the bias counter, as can be shown by simulations. After these 45 clock periods the final decision of $+1$ or -1 data detection can be taken. In case the bias counter does not reach at least a position of ± 6, the BER might be higher than 10^{-8}. This does not necessarily require 45 clock periods; several microsensor cells can run on the same track in parallel for data detection. If five micro sensor cells are running in parallel mode only $45/5=9$ clock periods are needed in this case. The quantization to binary signals is done very easily: if the bias counter has $b>0$ a binary 1 is decoded and if $b<0$ a binary 0; in the case of an odd decision number b cannot be zero. Let us assume a cell clock frequency of 20 MHz, five cells per track, and 16 parallel tracks detected on an integrated sensor allows a data stream of 20 MHz/9 cycles × 16 bit/2 breaks = 17.7 Mbit s^{-1}. Increasing the number of tracks running in parallel mode and increasing the clock frequency by 0.5 μm CMOS Si technology, far higher data streams for video applications are possible.

In general the error function given above is for binary data detection. A direct measure of the BER, if the complementary integral over the Gaussian distribution function is considered, can be expressed as follows:

$$BER=1-2\mathrm{erfc}(b_{Qm})=2\int_{b_{Qm}}^{\infty}\frac{1}{\sqrt{2\pi}}\exp\left(-\frac{1}{2}x^2\right)\mathrm{d}x \tag{25}$$

The accurate value, of course, is achieved without quantization by the integer function $b_{Qm}=2b_oL^{-1/2}$ with b_o being the position number of the bias counter.

Taking the inverse function, of course, the minimal number of clock periods for evaluation can be achieved.

4. The MAGFET detector circuit in Si CMOS

The magnetically sensitive region is a MOSFET enhancement channel of length l and width w with one common source, two separate drains at the end, and a joint gate which is clocked. The two drains are followed by a flip-flop circuit as shown in Fig. 3. When the joint channel is switched through by a clock signal the flip-flop falls into one of two possible stable states dependent on small starting-charge current differences at the MAGFET drains. This switching starts out of a currentless state. After the transient period one of the drains D4 or D5 has a low potential the other one a high potential. The information goes to the bias counter (not shown in the circuit). During the next phase the two drains of the MAGFET transistor have to be set at a defined potential again. Therefore two recharge transistors T2 and T3 are switched through while the clock signal itself is zero again. Small controllable voltage differences $U1_c$ and $U2_c$ at the end of the recharge transistors are used for symmetrization purposes.

A more complex circuit is shown by the self-calibrating magnetic field detector of Fig. 3. In this circuit the switching flip-flop consists of the transistors T2, T3, T4 and T5. The switching starts when the clock signal decreases. Small differences in the MAGFET channel during the transient phase decide the direction of switching. Such circuits cannot be fabricated symmetrically enough. Therefore a calibration is necessary to compensate the technological tolerances. Normally small fabrication symmetry deviations already have the consequence that a sole switching direction takes place in the equilibrium where no magnetic field is present. These symmetry deviations can be compensated electronically by increasing the current at the MAGFET drain side to which no switching is performed and when the device runs into saturation condition. A capacitance-controlled floating gate opens a resistive current and avoids the saturation. If, in addition, this saturation shift is measured by a floating voltage the total measuring range of the device can be increased. This self-calibration and range-increasing technique will be described in another contribution. Looking at Figs. 1 and 3 it should be mentioned that the sizes in the layout diagrams are not proportional to the real sizes. The logic-circuit diagram at the right side of Fig. 3 shows the functions of the different FETs.

4.1. Sensitivity of the digital MAGFET sensor

The sensitivity of such unknown microsensors is estimated roughly by FET models concentrating the point of interest on the Hall effect in the joint channel. The main results are confirmed, within reasonable fluctuations, by measurements carried out at similarly structured prototypes fabricated in CMOS [8].

The source for the decision within a MAGFET flip-flop is a small electron-flow difference to the two drains in the MAGFET channel given by the enhancement of electrons under the joint gate of transistor T1, see Fig. 3, during a very short start phase of the switching process within the flip-flop circuit T4, T5 and T1. The circuit is designed in such a way that during this switching start point the electrons in the channel

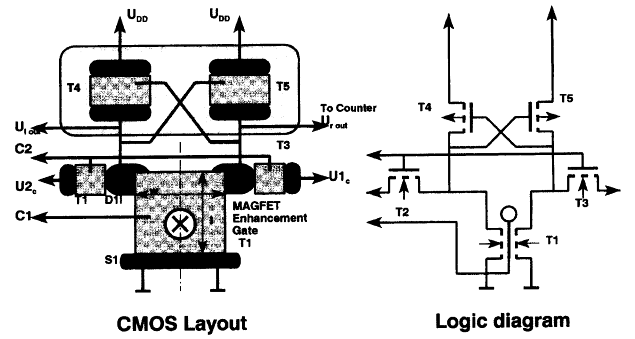

Fig. 3. Layout and logic diagram of the MAGFET transistor and flip-flop circuit.

can have a maximal speed given by $v_{\mathrm{emax}}=\mu_e E_{\max}$. According to the FET models, the electric field within the channel does not increase further if $U_{DS}\geq U_{GS}-U_{th}$, U_{th} being the threshold voltage of the channel. Therefore $U_{DS}=U_{GS}-U_{th}=U_{DSsat}$ defines the saturation voltage. It has to be taken into account that the charge density in the channel is higher at the source region and, consequently, the drift speed of electrons is not maximal. Only for $U_{DS}<U_{GS}-U_{th}$ is the charge density nearly constant, but in this case the electrical field is rather small. In the vicinity of the source in addition the short-circuit effect does not allow a transversal electric field because of the conductivity of the source region and its high carrier density. Therefore it is not efficient to achieve higher speed of electrons in this region.

For $U_{DS}\leq U_{GS}-U_{th}$ the current in the channel is estimated by

$$I_{DS}\simeq\frac{w}{l}\mu_e C_{ox}\left[(U_{GS}-U_{th})U_{DS}-\frac{1}{2}U_{DS}^2\right]$$

$$C_{ox}=\epsilon_r\epsilon_0\frac{wl}{d_{ox}} \qquad (26)$$

The maximal electric field in the channel corresponds to the saturation voltage. This gives the maximal mean speed of electrons, which is about 10^5 m s^{-1} for Si (and twice this for GaAs). The above charge-density difference in the channel gives an estimate of the effective velocity of electrons as $v_{\mathrm{eff}}=v_{\mathrm{emax}}/2\approx 0.5\times10^5$ m s^{-1}. To get the best transversal voltage in the channel generated by the magnetic field B (being orthogonal to the gate plate) the geometry coefficient $\mu_G=0.5$ has to be taken into account, arising from the finite size of drains and source. This leads to a voltage over the channel width w of

$$\delta u=\mu_G v_{\mathrm{eff}} wB\approx 0.25\times10^5 wB$$
$$=B\times 50\ \mathrm{mV\ T^{-1}}\ \text{for}\ w=2\ \mu\mathrm{m}$$

Similar values have been found in Ref. [6].

To consider the sensitivity, the amount of effective decisions caused by disturbing noise has to be estimated. The thermal noise energy in the channel, generated by the thermal movements of electrons, can be found by the directional resistance in the channel. The random thermal speed of the electron corresponds to the thermal energy $m_e v_T/2 = 3kT/2$, m_e being the mass of an electron, k the Boltzmann constant and T the Kelvin temperature. At 300 K this corresponds to an average speed of free electrons $v_T \approx 1.2 \times 10^5$ m s^{-1}, which is comparable to the speed generated by the electric field in silicon. Let R_l be the channel resistance in the length direction when the channel is switched through at a high level of U_{GS}. Then the thermal energy of this longitudinal direction corresponds to $E_{Tl} = 4kTR_l$. Let the transversal resistance be R_t. The channel might be virtually divided into left and right halves. The resistances for each half are $2R_l$ and $R_t/2$, respectively. Regarding the end of one half of the sliced channel, two transversal energies have to be superimposed: those of the left and right halves. Therefore the effective thermal noise energy for a virtual split channel will be $E_T = 4kT(2R_l + 2R_t/2)$. In addition to this channel noise, the feedback noise of the flip-flop transistor has to be added. It will be assumed that this is of the same value, which in total adds up to the energy $2E_T$. Hence the total noise amplitude can be estimated as: $\sigma = [2 \times 4kT(2R_l + R_t)f]^{1/2}$ where f denotes the frequency bandwidth considered. This corresponds to a sampling interval $\tau_s = 1/(2f)$.

The mean channel delay τ_c is estimated by the effective speed v_{eff} of electrons and the channel length l: $\tau_c = l/v_{eff} \approx 4 \times 10^{-11}$ s $= 0.04$ ns for $l = 2$ μm. Now let us assume the worst case, if a high feedback gain is used, that after two channel delays $2\tau_c$ it is principally the feedback loop that has produced the decision. This is equivalent to an effective noise voltage $\sigma = [2 \times 4kT(2R_l + R_t)/(2 \times 2\tau_c)]^{1/2}$. The typical resistance of Si for $l = w$ is $R_l = R_t = R \approx 1$ kΩ $= 10^3$ V A^{-1}. Thus we get the estimate $\sigma \approx [4kT \times 6R \times v_{eff}/4l]^{1/2} \approx 7.8 \times 10^4$ V $= 0.78$ mV. Other types of noise like shot noise or recombination noise are assumed to be negligible. This results in the following sensitivity for a 2 μm × 2 μm sensor plate:

$$\frac{\delta u}{\sigma} = \frac{B}{\beta} = B\mu_G v_{eff} w \frac{\sqrt{2l}}{\sqrt{4kT \times 6R \times v_{eff}}} \approx \frac{B}{15\ \text{mT}} \tag{27}$$

If such a device runs at a frequency of 16 MHz we can measure down to 7.5 μT every second.

The sensitivity of the special device given by Eq. (27) is only a rough performance estimation of a circuit layout which can be designed today. In a fabricated, but not yet optimized, structure we achieved a smaller sensitivity of about 20 mT running at a frequency of 20 MHz [9]. As the above-discussed best- and worst-case assumptions show, the sensitivity result can be improved by more optimized designs. Therefore the question of the sensitivity limit will be treated.

4.2. Absolute detection sensitivity

If the practical feasibility is neglected for a moment and only the theoretical barriers are considered, some of the worst-case assumptions can be removed immediately. For example, if an ideal detector is used for sampling in distances $\tau_s = 1/(2f_{Nyq})$ a counter can theoretically run at the frequency $f_c = 1/\tau_s$. This improves the sensitivity considerably. In addition geometrical design influences can be avoided. It can be assumed that the electrons in the enhancement channel have the maximal drift speed $v_{emax} \approx 10^5$ m s^{-1} for Si. Furthermore, we will set the theoretical prerequisite that a lot of separated sensor gate plates could be packed next to one another without spare areas in such a way that at a space of $NlMl$ μm^2 NM sensors could run in parallel at the highest Nyquist frequency. Then a virtual sensitivity can be defined with respect to an area in units of T μm^{-2}. We will assume that a quadratic Hall plate is at least necessary to measure the Hall voltage at the end. We know that the Hall voltage $U_H = v_e Bl$ increases linearly with the width l. Let a Hall plate be increased by the factor N. Then it covers an area which is $N2$ as large. On the other hand, there could run in parallel on the same area a multiple of N^2 stochastic detectors, giving N^2 decisions at the same time. That is to say, according to the stochastic rules applied above, the sensitivity of the sum of the detector cells is increased by the factor N, too.

Shortening the sampling interval τ_s by a factor $1/L^2$ statistically increases the sensitivity by the factor L. But at the same time the disturbing noise increases by the same factor. This allows the definition of a specific detector sensitivity per μm, per square-root temperature, and square-root seconds. This specific sensitivity will be a material constant defining the absolute magnetic-field detection barrier β_{m0} of the material. Eliminating geometrical influences and using theoretically optimal values only, we can calculate the following for $\delta u_{max}/\sigma_{min} = B/\beta_{minbar}$:

$$\beta_{minbar} = \beta_{0bar} \frac{\sqrt{A}\sqrt{T}}{\sqrt{f_c}}$$

$$\beta_{0bar} = \frac{\sqrt{4k \times 3R \times 2}}{v_{emax}} = 5.75 \times 10^{-15} \left[\frac{\text{T}}{\text{m}\sqrt{\text{K}}\sqrt{\text{s}}}\right] \tag{28}$$

At the temperature of 300 K this equation defines a minimal detectable magnetic field in silicon of

$$\beta'_{minbar} \approx 99\ \text{nT}\ (\text{Hz})^{1/2}\ \mu\text{m}^{-1}$$

That is to say: the absolute lowest detectable magnetic field on a 1 μm^2 silicon area is about 0.1 μT within one second measuring time at a temperature of 300 K. The error rate for this value is based on 0.32, corresponding to an argument value of one in the Gaussian error function.

5. Conclusions and application prediction

A stochastic principle has been applied to detect signals which are hidden in the noise. The very small signals to be discovered are generated by magnetic fields that are not deformed by the measurement; the method works without ferromagnetic materials. The posed problem of detecting small magnetic fields on a very small square-micrometre area has been solved by designing a directly digitizing double-drain MAGFET which discovers very small Hall fields by an unbalanced current in an enhancement FET channel. Together with a special flip-flop circuit, a bias counter and a quantization coder, a novel magnetic-field measurement device has been persented. The flexible high sensitivity opens new fields of magnetic micro-detection. The theoretically estimated magnetic detection barrier for silicon shows that potential optimization exists by semiconductor layout structuring and shrinking, even for a standard CMOS process. First prototypes of stochastic MAGFET cells have been fabricated and have confirmed some estimated and simulated results [10].

What types of new applications are possible? The main field is data detection in magnetic recording areas. As shown in Ref. [11], gigabit density recording has not yet reached its physical limits because of reading difficulties. Applying arrays of stochastic microsensor cells, this problem will be solved by digital reading track adaptation [12]. The density of hard disks can be increased considerably if the digital stochastic detection technique is used: eventually more than five times the amount of data can be stored on same area, of course, if separate reading and writing heads are installed. Reading a high number of tracks in parallel will increase the data stream dramatically for video applications. First estimations show that digital recording of 'Digital TV Studio Standard' will be possible on standard tapes.

Magnetic-field measurement devices can be improved by digital methods. Using three orthogonal stochastic microdetectors, three-dimensional measurement of small magnetic fields indicating the accuracy of their values and their directions will be possible.

Acknowledgements

The author, and the IPM Institute where some test chips have been designed, thank the DFG (Deutsche Forschungsgesellschaft) for sponsoring a research project in this field.

References

[1] N. Mathieu, P. Giordano and A. Chovet, Si MAGFETs optimized for sensitivity and noise properties, *Sensors and Actuators A, 32* (1992) 656–660.

[2] R.S. Popovic, *Hall Effect Devices — Magnetic Sensors and Characterization of Semiconductors*, Adam Hilger, Bristol, 1990.

[3] A. Nathan, K. Maenaka, W. Allegretto, H. Baltes and T. Nakamura, The Hall effect in integrated magnetotransistors, *IEEE Trans. Electron Devices, 36* (1989) 108–117.

[4] R. Gomez and A.A. Abidi, A 50 MHz CMOS variable gain amplifier for magnetic data storage systems, *IEEE J. Solid-State Circuits, 27* (1992) 935–939.

[5] R.K. Williams, A. Chang, M.E. Cornell and B. Concklin, Design and operation of a fully integrated BiC/DMOS head-actuator PIC for computer hard-disk drives, *IEEE Trans. Electron Devices, 38* (1991) 1590–1599.

[6] R.S. Popovic, A MOS Hall device free from short-circuit effect, *Sensors and Actuators, 5* (1984) 253–262.

[7] H.B. Baltes and R.S. Popovic, Integrated semiconductor magnetic field sensors, *Proc. IEEE, 74* (1986) 1107–1132.

[8] A. Nathan and H.P. Baltes, Integrated silicon magnetotransistors: high sensitivity or high resolution, *Sensors and Actuators, A21–A23* (1990) 780–785.

[9] S. Hentschke, A. Herrfeld and N. Reifschneider, Anti-alias Analog-digital-Wandlung mit rekursiver Rauschfilterung, *FREQUENZ, Zeit. für Telekommun., 46* (1992) 11–12.

[10] U. Barjenbruch, A novel highly sensitive magnetic sensor, *Sensors and Actuators A, 37–38* (1993) 466–470.

[11] Ching Tsang, Mao Min Chen and Tdashi Yogi, Gigabit-density magnetic recording, *Proc. IEEE, 81* (9) (1993).

[12] S. Hentschke and N. Reifschneider, A locally adaptive magnetic field detector, *IEEE Proc. 8th Int. ASIC Conf., Austin, TX, USA, 1995.*

Biography

Siebert Hentschke has been a full professor at the Kassel University (GhK) since 1984. He is responsible for 'digital engineering'. Currently he is also research fellow and director of the University IPM Institute. He graduated in electrical engineering and mathematics and received the Dr.-Ing. degree from the Technical University (TH) of Darmstadt in 1970 and 1972, respectively. He joined the SEL electronic company in Stuttgart, where he was responsible for R&D for new digital systems. He is one of the architects of the ISDN subscriber transmission system. He has published over 50 technical and scientific papers and patent applications. Besides his interest in the creation and design of new integrated digital devices for video computer systems, he is interested and successful in the design of 3D stereoscopic image-processing systems.